

Replica Tree-based Federated Learning using Limited Data

Ramona Ghilea^a, Islem Rekik^{a,*}

^a*BASIRA Lab, Imperial-X and Department of Computing, Imperial College London, London, UK*

Abstract

Learning from limited data has been extensively studied in machine learning, considering that deep neural networks achieve optimal performance when trained using a large amount of samples. Although various strategies have been proposed for centralized training, the topic of federated learning with small datasets remains largely unexplored. Moreover, in realistic scenarios, such as settings where medical institutions are involved, the number of participating clients is also constrained. In this work, we propose a novel federated learning framework, named *RepTreeFL*. At the core of the solution is the concept of a replica, where we replicate each participating client by copying its model architecture and perturbing its local data distribution. Our approach enables learning from limited data and a small number of clients by aggregating a larger number of models with diverse data distributions. Furthermore, we leverage the hierarchical structure of the clients network (both original and virtual), alongside the model diversity across replicas, and introduce a diversity-based tree aggregation, where replicas are combined in a tree-like manner and the aggregation weights are dynamically updated based on the

*Corresponding author: i.rekik@imperial.ac.uk, <http://basira-lab.com/>.

model discrepancy. We evaluated our method on two tasks and two types of data, graph generation and image classification (binary and multi-class), with both homogeneous and heterogeneous model architectures. Experimental results demonstrate the effectiveness and outperformance of *RepTreeFL* in settings where both data and clients are limited. Our code is available at <https://github.com/basiralab/RepTreeFL>.

Keywords: federated learning, limited data, replica, diversity

1. Introduction

Limited data has been an active area of research in machine learning, given that the performance of deep neural networks is highly dependent on the size of the dataset they are trained on. Different methods have been proposed to address this challenge, such as transfer learning (Torrey and Shavlik, 2010), data augmentation (Shorten and Khoshgoftaar, 2019), and more recently, generating synthetic samples using Generative Adversarial Networks (GANs) (Goodfellow et al., 2020). However, applying these techniques where data resides on different devices is not straightforward.

Federated Learning (Kairouz et al., 2021) is an approach that can be applied in the setting where data is spread across multiple machines, as it aggregates a set of models with different datasets without compromising the data privacy. While various challenges in federated learning have been analysed, such as differences in data distributions across clients (Li et al., 2020; Acar et al., 2020; Hanzely and Richtárik, 2020; Deng et al., 2020; Sattler et al., 2020; Ghosh et al., 2020; Arivazhagan et al., 2019; Zhang et al., 2021) or model heterogeneity (Horvath et al., 2021; Diao et al., 2020; Caldas et al.,

2018; Alam et al., 2022; Shamsian et al., 2021; Litany et al., 2022; Li and Wang, 2019; He et al., 2020), the limited data issue has not been addressed often. Furthermore, federating a small number of models, which is the case in specific real-world scenarios, is largely unexplored. Therefore, the key research question becomes: *How can we learn efficient models in federated learning in a setting where both data and the participating clients are limited?*

In this work, we propose a new federated learning method which enables the learning from limited data with only a small number of participating clients, named *RepTreeFL*. In this setting, each client is replicated for a number of times and the original data distribution is modified at each replica, which acts as a virtual copy of the client. The underlying idea is that a greater number of clients with diverse data distributions could enhance the ability of the global model to generalize. However, in real-world scenarios where medical data and healthcare institutions are involved, the number of participating hospitals (clients) is often limited and their local datasets have small sizes. Beyond replicating only the original clients, replicas creation can be done recursively, such that a replica of a replica is created, in order to obtain an even larger amount of diverse models. By leveraging the tree structure of the original and virtual clients and the model diversity across replicas, we introduce a diversity-based tree aggregation, where replicas are aggregated in a tree-like manner and the aggregation weights are dynamically computed based on the discrepancy between models. We evaluate the solution in two different settings: graph generation with heterogeneous models (where architectures vary in dimension) and image classification (binary and multi-class) with homogeneous models. The replica-based federation was

published originally in our previous work (Ghilea and Rekik, 2023). This paper extends our earlier work with the following contributions:

1. We propose a novel diversity-based tree aggregation, which leverages the tree structure of the client network and the model diversity across replicas to enhance the model performance.
2. We introduce a new hyperparameter to the framework: the tree depth at the client level. In the proposed method, replicas can be created at varying depths, generating a tree of models with multi-length pathways.
3. Beside the graph super-resolution task, we evaluate both RepFL (Ghilea and Rekik, 2023) and RepTreeFL on a secondary task: image classification. Therefore, we demonstrate the efficacy of the proposed method in a limited data setting with a small number of participating clients on two tasks and two types of data. Additionally, we evaluate the framework using homogeneous and heterogeneous model architectures.

2. Related Work

2.1. Learning from small datasets

Extensive research has been conducted in machine learning to address the challenge of learning from limited data, as collecting large, high-quality datasets is impractical in general. One technique that was proposed to address this issue is transfer learning (Torrey and Shavlik, 2010; Zhuang et al., 2020; Kim et al., 2022). This approach aims to enhance learning for a target task by leveraging knowledge acquired from a source task. For instance, a model can be initially trained on a large dataset, then the learned weights can be used as a starting point for a new task which requires a much smaller

dataset. Another solution is data augmentation, which overcomes the limitation by modifying the training dataset (Shorten and Khoshgoftaar, 2019; Chlap et al., 2021). In the context of images, a straightforward approach to augment the data involves applying simple transformations such as rotation, flipping, or cropping. A more recent technique is data synthesis, which can also be viewed as a form of data augmentation. This method consists in generating synthetic data that has similar characteristics to the original training dataset. These new samples can be created using generative models such as Generative Adversarial Networks (GANs) (Goodfellow et al., 2020; Gui et al., 2021). However, these approaches face various challenges when applied in the federated learning setting, as data augmentation could only be conducted on the local samples, transfer learning requires a public dataset, while GANs need a considerable amount of samples in order to generate high quality outputs.

2.2. Federated Learning

Federated Learning is an approach that enables multiple clients to collaborate and train a global model without sharing their local datasets (Kairouz et al., 2021). In this way, models residing on different devices benefit from training from a larger amount of samples while preserving the data privacy. The classic federated learning algorithm is FedAvg (McMahan et al., 2017), where clients train their local models for multiple epochs and the server averages their parameters at each round. Later, a wide range of proposed methods addressed different challenges in federated learning.

One of the main limitations in federated learning is the difference between data distributions across clients. Li et al. proposed FedProx (Li et al., 2020),

which introduces a additional term to the local objective and penalizes parameters that are at a considerable distance from the global model. FedDyn (Acar et al., 2020) adds a similar regularisation term, encouraging parameters of client models to converge to global stationary points. A large category of frameworks that address the data heterogeneity issue is personalized federated learning (Kulkarni et al., 2020; Tan et al., 2022). In this setting, instead of training a single global model, each client generates a personalized model that addresses its own requirements. Model mixing is a popular approach in personalized federated learning (Hanzely and Richtárik, 2020). For instance, APFL (Deng et al., 2020) aims to identify the optimal combination of global and local models using a client-specific parameter. Clustered federated learning was also proposed to create personalized models and consist in grouping similar clients and generating a different model for each group. (Sattler et al., 2020) introduces hierarchical clustering, where the server recursively creates two clusters of clients by minimising the cosine similarity between models from the two different groups. In a distinct work (Ghosh et al., 2020), where the number of clients is fixed, the clients are assigned a cluster at each round. (Arivazhagan et al., 2019) created FedPer, where the global model is split into base and personalized layers. While the base layers undergo training via federated averaging, the personalized layers are trained exclusively utilizing the local dataset. A specific type of personalization was proposed in (Zhang et al., 2021), where each client federates with other relevant clients.

Other studies focused on federating models with different architectures, where aggregation becomes more challenging. Partial training of the global model was one of the first proposed ideas (Horvath et al., 2021; Diao et al.,

2020) for solving this problem. An example from this category is Federated Dropout (Caldas et al., 2018), which involves setting a subset of the activations to zero in each layer of a client network. Next, only the remaining neurons are trained and transmitted to the server in a federation round. FedRolex (Alam et al., 2022) suggested an innovative rolling window extraction of the sub-models for aggregation. The window advances in each round and selects a different part of the global model each time, resulting in a uniform training of the server model parameters. Another set of works developed hypernetworks to generate the personalized model weights. pFedHN (Shamsian et al., 2021) was initially created for solving the data heterogeneity limitation, but it was also evaluated on models with heterogeneous architectures. The solution uses such a hypernetworks to create weights for each client individually using client embeddings. Graph hypernetworks (Litany et al., 2022) were later proposed, which operate on the graph representation of the client architecture. Knowledge distillation (Hinton et al., 2015) was also applied as a solution for federating heterogeneous architectures. FedMD (Li and Wang, 2019) firstly performs transfer learning, as each client trains its model on a public dataset and then on its private dataset, the during the federation, the knowledge is transferred form server to clients. Another study (He et al., 2020) introduces group knowledge transfer, where knowledge is transferred bidirectionally between clients and server.

While learning from limited data has been extensively studied in machine learning, federated learning with small datasets has been underexplored. One study (Li and Wang, 2019) considers it as a secondary challenge and applies transfer learning to address it, while another work (Kamp et al., 2022) pro-

poses permutations of the local models as a solution. However, while the former requires a public dataset, the latter may raise privacy concerns, as models are transferred across clients during federation. Moreover, we are also interested in learning with a few participating clients. We previously developed a replica-based federated learning solution for the limited data setting with a small number of participating clients (Ghilea and Rekik, 2023). However, we extend the approach presented in our earlier work by taking into account the diversity across models in the aggregation step and making the depth of the replicas variable across clients.

3. Method

3.1. Problem Formulation

The goal of federated learning is to train and aggregate m clients, where each client has access to its local dataset D_i . In RepTreeFL¹, there are m original clients and each client is replicated for r_i times, where i is the index of the client. The original clients are denoted by *anchors* and the virtual copies of these clients as *replicas*. While the model architecture of the replica is identical to the one on the anchor, the dataset is slightly modified, as the original data distribution is perturbed. The perturbation consist in removing a small percentage p_i of samples from the original dataset. We previously described the idea of replicating the original clients in federated learning in (Ghilea and Rekik, 2023).

Moreover, we introduce a new concept: a replica can also have its own

¹<https://github.com/basiralab/RepTreeFL>

replicas, creating a tree of anchors and replicas. The depth of each anchor is controlled by hyperparameter d_i and each replica of a replica is created in the same way as a replica of an anchor, by copying the model architecture and perturbing the dataset of the parent replica this time. Finally, we federate $m + \sum_{i=1}^m (r_i + r_i^2 + \dots + r_i^{d_i})$ models.

The idea is illustrated in Figure 1. Client h_i is replicated for r_i times, then each of its replicas creates its own replicas, resulting in a tree of models. The model architecture is copied at each replica level, while a subset of samples are removed from the parent client.

In our RepTreeFL, the aggregation is performed at each parent node and the aggregation weights are dynamically generated based on a model diversity metric. The local dataset D_i of client i contains n_i samples. For the classification task, each sample is represented by the image $X_{i,j}$ and the label $y_{i,j}$, where j is the j th sample of client i . In contrast, for the generation task, each sample is represented by a low-resolution (LR) source graph $X_{i,j}^s$ and a high-resolution (HR) target graph $X_{i,j}^t$ (with higher resolution than the source graph resolution). Appendix Table A.5 summarizes all the mathematical notations used in this work.

3.2. RepTreeFL: Replica-based Federated Learning

3.2.1. Replica

At the core of our solution is the concept of a replica, introduced in (Ghilea and Rejik, 2023). One limitation that exists in some specific federated learning situations, such as when medical institutions are involved, is the small number of clients that can participate in the federation. The replication of the original clients generates a larger amount of clients, which overcomes

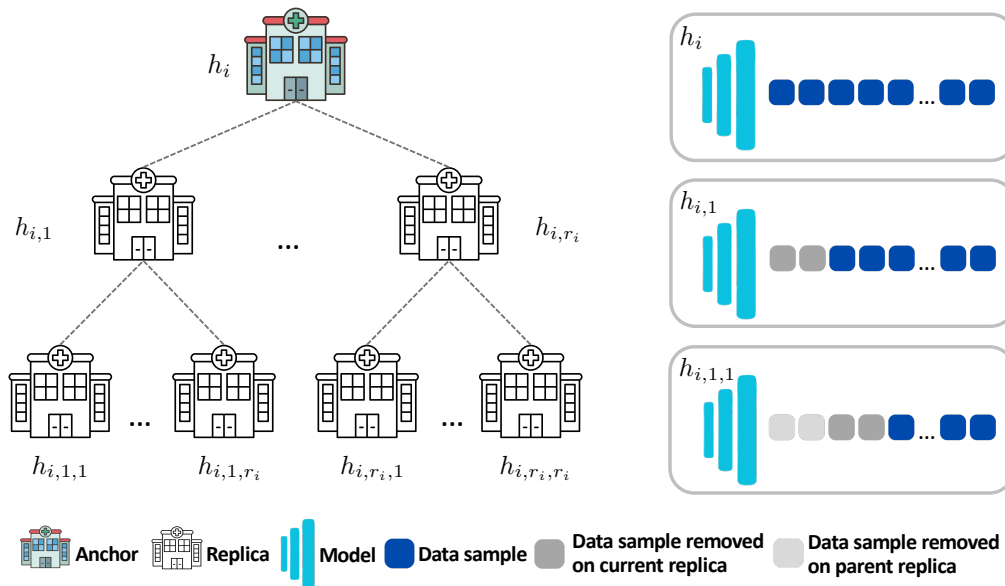


Figure 1: Anchor i and its replicas with $d_i = 2$. h_i is an anchor hospital (client), $h_{i,1}$ is its first replica and $h_{i,1,1}$ is the first replica of the replica $h_{i,1}$. At each replica, the model architecture is copied from the parent, while the dataset of the parent is perturbed.

this challenge. A second limitation that exists in real-world scenarios is the small amount of data. The solution for this challenge is closely related to the client replicas, as on each virtual client, a slightly different local dataset is created by perturbing the parent (anchor or replica) data distribution. The intuition is that a larger amount of clients with diverse data distributions would enhance the generalisability of the global model. The replica creation is defined by two key aspects:

- **Model architecture:** the replica model is identical to the parent model
- **Dataset:** the data distribution of the parent local dataset is perturbed

on the replica by removing a small percentage of the samples

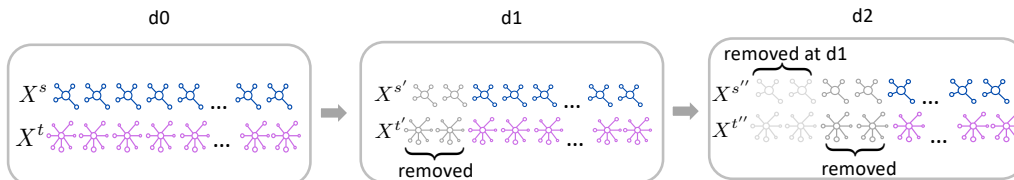


Figure 2: Perturbation of the data distribution at the anchor and replicas with $d_i = 2$.

The hierarchical perturbation of the data distribution for the graph generation task is illustrated in Figure 2. At each replica at level $d = 1$, a small amount of samples is removed from both the set of source graphs X^s and the set of target graphs X^t at the anchor, resulting in the new dataset consisting of the source graphs $X^{s'}$ and the set of target graphs $X^{t'}$. Furthermore, for each instance of an anchor, the removed samples will vary. For example, if at replica l of client i , where the perturbation rate is $p_i = 10\%$ and the dataset size is $n_i = 20$, samples with indices j and $j + 1$ are excluded, at the subsequent replica $l + 1$ from the same client, the samples with indices $j + 2$ and $j + 3$ will be excluded. If the depth d_i of the current anchor is 2, at each replica at level $d = 2$, a small amount of samples is removed from the sets of graphs $X^{s'}$ and $X^{t'}$ at the replica at the previous level, resulting in the new dataset consisting of the set of source graphs $X^{s''}$ and the set of target graphs $X^{t''}$.

3.2.2. Diversity-based Aggregation

We aim to boost the diversity across the generated replicas to enhance the model performance. To achieve this, we propose a model discrepancy metric to quantify the dissimilarity between the anchor model and each of

its replicas. Similarly, the metric can be computed if the parent node is a replica itself. The model diversity is computed as follows:

$$div(a, r) = \frac{1}{n_c} \sum_{k=1}^{n_c} divMetric(a_k, r_k)$$

where n_c is the number of aggregated layers, k is the layer index, a is an anchor and r is a replica of anchor a . $divMetric$ can be any metric that can quantify the dissimilarity between two layers.

Specifically, we apply the L2 norm to measure the distance between the same layer belonging to two different models. The L2 norm between two layers is computed as follows:

$$\|a_k - r_k\|_2 = \sqrt{\sum_{l=1}^L (a_k^l - r_k^l)^2}$$

where l is the index of an element in the weight matrix of the layer k and L is the size of the layer.

Finally, we compute the normalized weights α for replica aggregation based on the diversity metric. In this approach, replica models which are at a larger distance from the anchor model receive greater weights. Given that the anchor is trained on a larger dataset compared to its replicas, we assign it a larger weight for the final anchor model:

$$a \leftarrow \frac{1}{2} \left(\sum_{r=1}^{r_i} \alpha_r \times r_r + a \right)$$

where α_r is the previously computed weight for replica r and r_i is the number of replicas for the current anchor.

The steps taken in the diversity-based tree aggregation are listed in Algorithm 1.

Algorithm 1 *Diversity-based Tree Aggregation.* i is the anchor index; r_i is the number of replicas for anchor i ; $divArray$ is an array which stores the diversity values between the anchor i and each of its replicas; div is a function which computes the discrepancy between two models;

aggregateDiversity(i):

for $r = 1$ **to** r_i **do**

$divArray_r \leftarrow div(a_i, r)$

end for

$\alpha \leftarrow \text{computeDivAggregationWeights}(divArray)$

$W_{t+1,i} \leftarrow \frac{1}{2}(\sum_{r=1}^{r_i} \alpha_r \times W_{t+1,r} + W_{t+1,i})$

3.2.3. *RepTreeFL*

The pseudocode of *RepTreeFL* is described in Algorithm 2. At the beginning, each anchor instantiates its replicas, then replicas of replicas are created, according to the depth d . Afterwards, at each round, the anchor is trained alongside its virtual copies and the replicas are aggregated hierarchically, at the parent node level, using the dynamically generated weights. Considering that there is a small number of clients, all of them are participating at each round. Finally, the server aggregates the anchors as in classic federated learning.

Algorithm 2 *RepTreeFL*. There are m clients indexed by i ; E is the number of local epochs; R is the number of rounds; B_i is the number of local minibatches on client i , where the local dataset was split into minibatches of size B ; r_i is the number of replicas for client i ; d_i is the depth for client i ; η is the learning rate;

```

1: INPUTS:
    $D_{i,j} = \{X_{i,j}, y_{i,j}\}$ : image and label of the  $j^{th}$  subject in local dataset  $D_i$  of client  $i$ 

2: Server executes:
3:   for each client  $i = 1$  to  $m$  do
4:     createReplicas( $i, r_i, d_i$ )
5:   end for
6:   for each round  $t = 1$  to  $R$  do
7:     for each client  $i = 1$  to  $m$  do
8:        $W_{t+1,i} \leftarrow$  clientUpdate( $i, W_{t,i}$ )
9:     end for
10:     $W_{t+1} \leftarrow \frac{1}{m} \sum_{i=1}^m W_{t+1,i}$ 
11:  end for

12: createReplicas( $i, repNo, depth$ ):
13:   if  $depth > 0$  then
14:     for  $r = 1$  to  $repNo$  do
15:       createReplicas( $r, repNo, depth - 1$ )
16:     end for
17:   end if

18: clientUpdate( $i, W_t$ ):
19:   for each local epoch  $e = 1$  to  $E$  do
20:     for each minibatch  $b = 1$  to  $B_i$  do
21:        $W_{t+1} \leftarrow W_t - \eta \nabla l(W_t, b)$ 
22:     end for
23:   end for
24:   if hasReplicas( $i$ ) then
25:     for each replica  $r = 1$  to  $r_i$  do ▷ run one round for each replica
26:        $W_{t+1,r} \leftarrow$  clientUpdate( $r, W_{t,r}$ )
27:     end for
28:      $\alpha \leftarrow$  computeDivAggregationWeights( $i$ )
29:      $W_{t+1,i} \leftarrow \frac{1}{2} (\sum_{r=1}^{r_i} \alpha_r \times W_{t+1,r} + W_{t+1,i})$ 
30:   end if
31:   return  $W_{t+1}$ 

```

3.3. RepTreeFL with Heterogeneous Models

There are cases in federated learning where model architectures are different across clients. For instance, clients might have different compute capacities or they might focus on different tasks, such as in multi-tasking. In this case, models are heterogeneous and only a subset of the layers are common across architectures. We adapt the federation in the heterogeneous models setting by federating only the common layers, while training the personalized layers only locally, as in (Diao et al., 2020). The local parameter update is described in Algorithm 3. After the training of replicas, the common layers W^C are aggregated at the parent node level (i.e., anchor or replica on the level above) and then sent to the server.

Algorithm 3 *Parameter Update for Heterogeneous Models.* i is the client index; E is the number of local epochs; R is the number of rounds; B_i is the number of local minibatches on client i , where the local dataset was split into minibatches of size B ; η is the learning rate;

```
1: for each local epoch  $e = 1$  to  $E$  do
2:   for each minibatch  $b = 1$  to  $B_i$  do
3:      $W^C \leftarrow W^C - \eta \nabla l(W^C, b)$   $\triangleright$  update the common (federated) layers
4:      $W_i^D \leftarrow W_i^D - \eta \nabla l(W_i^D, b)$   $\triangleright$  update the personalized layers on client  $i$ 
5:   end for
6: end for
```

4. Experiments

4.1. Datasets and Models

We evaluate the performance of RepTreeFL in two settings: on image classification with homogeneous models and on graph super-resolution with heterogeneous models.

For the image classification task, two datasets from the MedMNIST benchmark (Yang et al., 2021, 2023) were selected: PneumoniaMNIST for binary classification and OrganCMNIST for multi-class classification (Bilic et al., 2019; Xu et al., 2019). Given that our method is developed for limited data setting, we evaluate the framework on a subset of the train set, such that each client has a local dataset of 200 samples. As model architecture, we use ResNet10, a smaller variant of the well-known ResNet18 architecture (He et al., 2016). In this task, all layers are federated, considering that the clients have the same model architecture.

For the graph super-resolution task, we used a brain graph dataset derived from the Southwest University Longitudinal Imaging Multimodal (SLIM) Brain Data Repository (Liu et al., 2017) using the parcellation approaches described in (Dosenbach et al., 2010) and (Shen et al., 2013). This dataset contains 279 subjects represented by three brain connectomes: a morphological brain network with resolution 35 (where the resolution denotes the number of brain regions or nodes) derived from T1-weighted MRI, a functional brain network with resolution 160 derived from resting-state functional MRI and a functional brain network with resolution 268 derived from resting-state functional MRI. Further information about the multi-resolution brain graph dataset is available at (Cinar et al., 2022). The models in this setting

Table 1: Dataset statistics

Dataset	Task (No. Classes)	Size	Selected Subset	Client Dataset
SLIM (Liu et al., 2017)	Graph Genera- tion	279	279	55
PneumoniaMNIST (Yang et al., 2021, 2023)	Binary-Class(2) Classification	4,708	800	200
OrganCMNIST (Yang et al., 2021, 2023; Bilic et al., 2019; Xu et al., 2019)	Multi-Class(11) Classification	13,000	800	200

can have one of two architectures: G_1 , which takes as input a morphological brain connectome of resolution 35 and outputs a functional brain graph of resolution 160, or G_2 , which takes as input a morphological brain connectome of resolution 35 and outputs a functional brain graph of resolution 268. Both models have an graph neural network (GNN) encoder-decoder architecture, which contains edge-based graph convolutional network (GCN) layers (Simonovsky and Komodakis, 2017) and implement the mapping function defined in SG-Net (Mhiri et al., 2021), which creates a symmetric brain graph ². Given that clients have heterogeneous architectures, the parameter update with common and personalized layers described previously is used.

²The mapping function and graph preprocessing steps were implemented using code from <https://github.com/basiralab/SG-Net>.

The statistics of the datasets are listed in Table 1.

4.2. Baselines

We compare RepTreeFL against the standalone version (where no federation is applied) and four other federated learning algorithms: FedAvg (McMahan et al., 2017), FedDyn (Acar et al., 2020), FedDC (Kamp et al., 2022) and RepFL (Ghilea and Rekik, 2023). Details of the baselines are presented below.

Standalone refers to the setting where each client is trained exclusively on its own local dataset and no federation is performed.

FedAvg (McMahan et al., 2017) is the first federated learning algorithm proposed and the most widely applied. In each round, clients train their local models for multiple steps, then communicate their updates to the server, the server computes the average of all received parameters and transfers the new average to the clients.

FedDyn (Acar et al., 2020) extends FedAvg (McMahan et al., 2017) by introducing a dynamic regularizer to the local objective. It addresses the limitation of statistical heterogeneity across clients while reducing the communication costs.

FedDC (Kamp et al., 2022) is a solution specifically developed for federated learning with limited data. The approach consist in transferring models across clients and training them on the other clients local datasets.

RepFL (Ghilea and Rekik, 2023) is our previously proposed federated learning framework for the limited data setting with a small amount of clients. It is a simpler version of RepTreeFL, where the depth is set to $d = 1$ and

a simple aggregation is performed (i.e. all anchors and replicas are assigned the same weights for aggregation).

For the graph super-resolution task, where the models have heterogeneous architectures, FedAvg, FedDyn and FedDC were adapted and applied only on the common layers.

4.3. Experimental Setup

For image classification, the number of clients is set to three. In the graph generation setting, four clients are used: two clients with the target resolution 160 and two clients with the target resolution 268. The datasets are split between clients in order to simulate the federated learning setting. The framework is evaluated using four fold cross-validation in the image classification setting and five fold cross-validation in the second setting. For each fold configuration, each client receives one fold as its local dataset and the remaining fold is used as a global test set. For both tasks, the number of local epochs is set to $E = 10$ and the number of rounds is $R = 10$. For FedDyn, α is set to 0.01, for FedDC, the daisy-chaining period is 1, and in RepFL, we keep the same perturbation rate and number of replicas as in the proposed method. For image classification, the batch size is 20, the learning rate is set to 0.005 for PneumoniaMNIST (Yang et al., 2021, 2023) and to 0.001 for OrganCMNIST (Yang et al., 2021, 2023; Bilic et al., 2019; Xu et al., 2019). The optimizer for PneumoniaMNIST is SGD and for OrganCMNIST we use Adam. The loss function applied is cross-entropy loss. For graph generation, a batch size of 5 is used, the learning rate is set to 0.1, SGD is used as optimizer and as loss function, the L1 loss is applied. For simplicity, we fix the number of replicas r , the perturbation rate p and the depth d

across clients, but they can be variable.

4.4. Performance comparison to baselines

The comparison to baseline methods in the image classification task can be seen in Tables 2 and 3 and in the graph super-resolution task in Table 4. We report the accuracy, F1 score, sensitivity and specificity on the image classification task, and the mean absolute error (MAE) in the graph generation task. The values are reported for each client model on the global test set across four and five folds, respectively. Additionally, the accuracy comparison in image classification is shown in Figure 3 and the MAE in graph generation is illustrated in Figure 4.

First, the federated learning algorithms show significant performance gain compared to the standalone version on both tasks and on all three datasets. These results demonstrate that federated learning enables the clients to efficiently collaborate and benefit from complementary knowledge, which is especially important when the local datasets are small.

Second, the proposed method, RepTreeFL, generally outperforms all baselines in both settings, image classification (both binary and multi-class) with homogeneous models and graph generation with heterogeneous models. The only exception is hospital (client) H2 on the PneumoniaMNIST (Yang et al., 2021, 2023) dataset, where RepFL (Ghilea and Rejik, 2023), our previously developed method, reaches slightly better results across all metrics. Moreover, RepTreeFL achieves the smallest standard deviation across folds on both tasks and all datasets.

Table 2: Comparison to baselines on PneumoniaMNIST

Method	H1				H2				H3			
	Acc	F1	Sens	Spec	Acc	F1	Sens	Spec	Acc	F1	Sens	Spec
Standalone	93.24	91.18	91.34	91.34	92.99	90.80	90.69	90.69	93.49	91.42	91.20	91.20
FedAvg	94.11	92.31	92.40	92.40	94.24	94.24	94.24	92.80	94.86	93.28	93.22	93.22
FedDyn	93.87	91.96	92.08	92.08	94.37	92.70	92.88	92.88	94.99	93.46	93.46	93.46
FedDC	94.62	92.94	92.73	92.73	94.62	93.05	93.66	93.66	94.37	92.70	93.03	93.03
RepFL (ours)	96.37	95.22	94.87	94.87	96.62	95.57	95.51	95.51	96.12	94.85	94.22	94.22
RepTreeFL (ours)	96.62	95.56	95.36	95.36	96.50	95.40	95.27	95.27	96.37	95.18	94.54	94.54

Table 3: Comparison to baselines on OrganCMNIST

Method	H1				H2				H3			
	Acc	F1	Sens	Spec	Acc	F1	Sens	Spec	Acc	F1	Sens	Spec
Standalone	63.56	58.28	57.85	96.19	66.33	63.21	62.65	96.48	63.56	59.23	58.17	96.19
FedAvg	74.53	71.66	70.64	97.35	75.66	73.72	72.08	97.46	75.54	73.14	72.36	97.48
FedDyn	73.27	70.52	69.39	97.22	74.91	72.78	71.21	97.38	75.16	72.94	72.12	97.45
FedDC	79.95	78.48	77.61	97.93	81.46	79.52	79.26	98.10	81.59	80.26	79.78	98.10
RepFL (ours)	82.47	79.58	80.13	98.24	82.59	80.12	79.94	98.22	83.23	80.90	80.79	98.31
RepTreeFL (ours)	83.73	81.14	81.31	98.36	84.86	82.61	82.83	98.47	84.24	82.17	82.06	98.41

4.5. Analysis of the perturbation rate, depth and the diversity-based aggregation

Additionally, we study the influence of two hyperparameters on the framework performance, the rate of perturbation p and the depth d . Also, we compare our method, which applies diversity-based aggregation, with simple aggregation, where the replica federation is performed with fixed weights and all clients (original and virtual) are assigned the same weight when aggregated. We analyse the values $p \in \{10\%, 20\%, 30\%\}$ and $d \in \{1, 2, 3\}$. We fix the number of replicas to $r = 3$. We conduct this experiment on Pneu-

Table 4: Comparison to baselines on SLIM

Method	H1	H2	H3	H4
Standalone	0.1804 ± 0.0038	0.1804 ± 0.0039	0.2230 ± 0.0051	0.2229 ± 0.0053
FedAvg	0.1719 ± 0.0034	0.1719 ± 0.0035	0.1964 ± 0.0045	0.1963 ± 0.0046
FedDyn	0.1720 ± 0.0034	0.1720 ± 0.0035	0.1964 ± 0.0045	0.1962 ± 0.0046
FedDC	0.1718 ± 0.0034	0.1720 ± 0.0034	0.1959 ± 0.0046	0.1957 ± 0.0049
RepFL (ours)	0.1706 ± 0.0033	0.1706 ± 0.0033	0.1931 ± 0.0043	0.1931 ± 0.0041
RepTreeFL (ours)	0.1687 ± 0.0024	0.1684 ± 0.0021	0.1839 ± 0.0036	0.1841 ± 0.0029

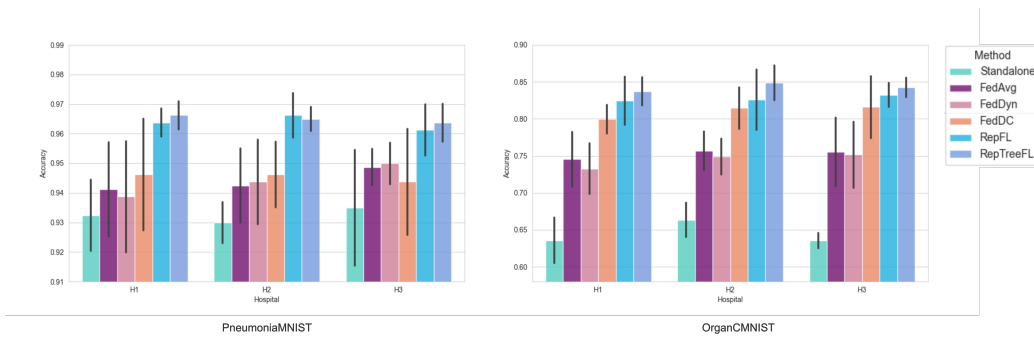


Figure 3: Accuracy on PneumoniaMNIST and OrganCMNIST. H1, H2 and H3 are clients (hospitals) having the same model architecture. Perturbation rate is $p = 10$, number of replicas is $r = 3$ and depth is $d = 1$.

moniaMNIST (Yang et al., 2021, 2023). Figure 5 illustrates our comparative analysis. The simple aggregation version with $d = 1$ is equivalent to RepFL (Ghilea and Rezik, 2023).

Firstly, while the version with simple aggregation, depth $d = 2$ and perturbation rate $p = 10\%$ outperforms the other variants for one client, the difference in accuracy compared to RepTreeFL with depth $d = 1$ is negligible. Therefore, in this setting, the ideal depth is $d = 1$, considering that another level of replicas implies additional computation and memory costs.

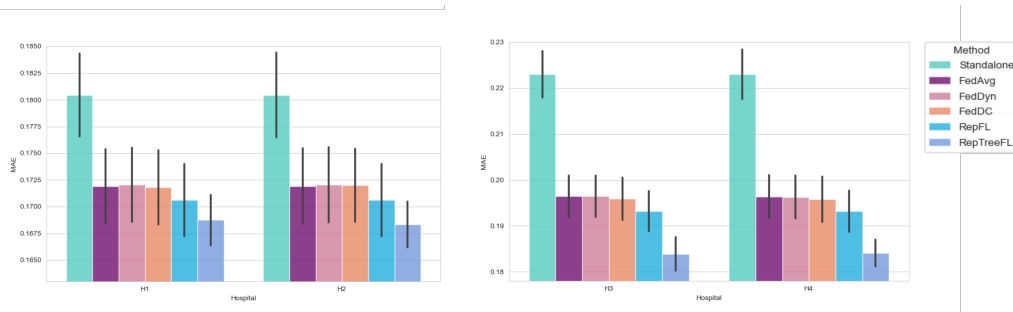


Figure 4: Mean Absolute Error (MAE) on SLIM. Clients H1 and H2 have as super-resolution GNN model G_1 , while clients H3 and H4 have architecture G_2 . Perturbation rate is $p = 10$, number of replicas is $r = 5$ and depth is $d = 1$.

Secondly, the diversity-based tree aggregation version outperforms the simple aggregation in most of the cases, which proves the efficacy of the proposed aggregation approach.

4.6. Analysis of the perturbation approach

Next, we analyse the perturbation approach on PneumoniaMNIST (Yang et al., 2021, 2023) and compare the stratified perturbation to random perturbation on RepFL (Ghilea and Rekik, 2023) and the proposed method. In stratified perturbation, when removing a subset of samples on each replica, we maintain the same label distribution as in the anchor dataset. We fix the rate of perturbation to $p = 10\%$, the number of replicas to $r = 3$ and the depth to $d = 1$. Figure 6 shows that RepTreeFL achieves better results when the stratified approach is applied. Moreover, RepFL (which involves simple aggregation) with stratified perturbation outperforms RepTreeFL with random perturbation, which proves the importance of perturbing the local datasets by preserving the label distribution of the anchor dataset.

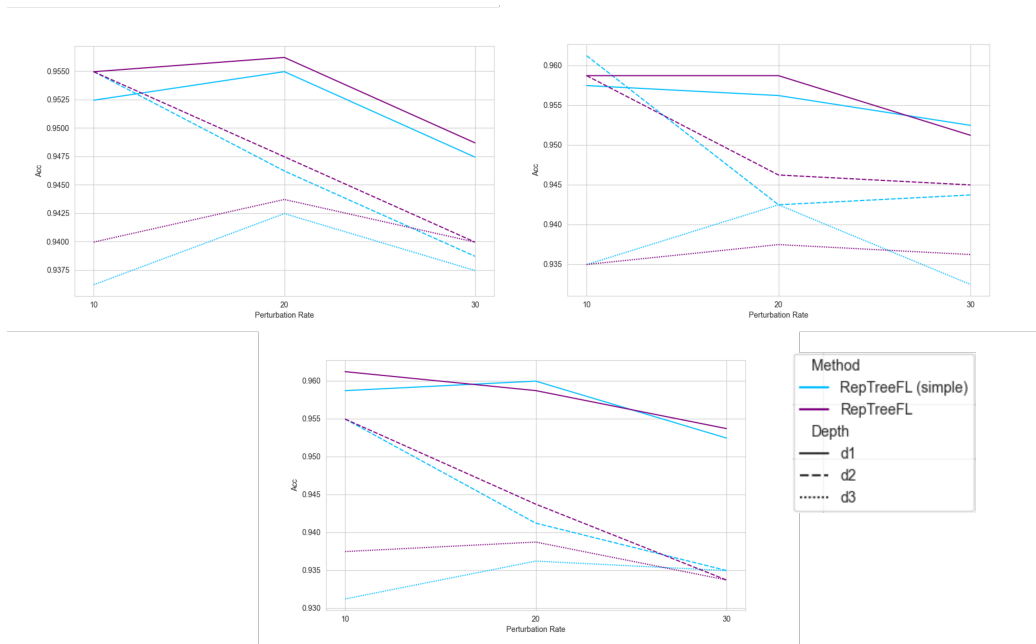


Figure 5: Accuracy analysis of the the rate of perturbation and depth on PneumoniaMNIST. Number of replicas is $r = 3$.

4.7. Performance on smaller datasets

As our solution is developed for a setting where data is limited, we study the behaviour of RepTreeFL on smaller subsets of PneumoniaMNIST (Yang et al., 2021, 2023) and compare it to the baselines. We analyse the dataset size values $n \in \{20, 100, 200\}$. The rate of perturbation is set to $p = 10\%$, to ensure that very small local datasets do not suffer from a significant reduction in the number of removed samples. We also fix the number of replicas to $r = 3$ and the depth to $d = 1$. It can be observed in Figure 7 that our method outperforms on average the other federated learning methods on local datasets of various small sizes.

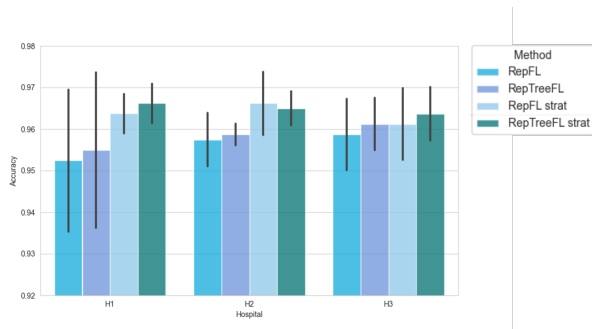


Figure 6: Accuracy analysis of the perturbation approach on PneumoniaMNIST. Perturbation rate is $p = 10\%$, number of replicas is $r = 3$ and depth is $d = 1$.

4.8. Comparison to centralized training

We compare the proposed method to the centralized training setting, where a model is trained using all samples, which were distributed across clients in the federated learning setting. The evaluation is performed using four fold cross-validation for image classification and five fold cross-validation for graph generation, as in the previous experiments. For each configuration in the centralized training setting, three (or four) folds are used for training, and the remaining fold is used for testing. The results for image classification and graph generation can be observed in Figures 9 and 8, respectively.

Although RepFL (Ghilea and Rekik, 2023) and RepTreeFL demonstrate accuracy levels similar to centralized training on OrganCMNIST (Yang et al., 2021, 2023; Bilic et al., 2019; Xu et al., 2019), they surpass centralized training when applied to PneumoniaMNIST (Yang et al., 2021, 2023). A better performance on PneumoniaMNIST than on OrganCMNIST is expected, as the binary classification task in PneumoniaMNIST is considered easier compared to the multi-classification task in OrganCMNIST. The gain in accuracy of RepTreeFL over centralized training can be explained by the boosting ef-

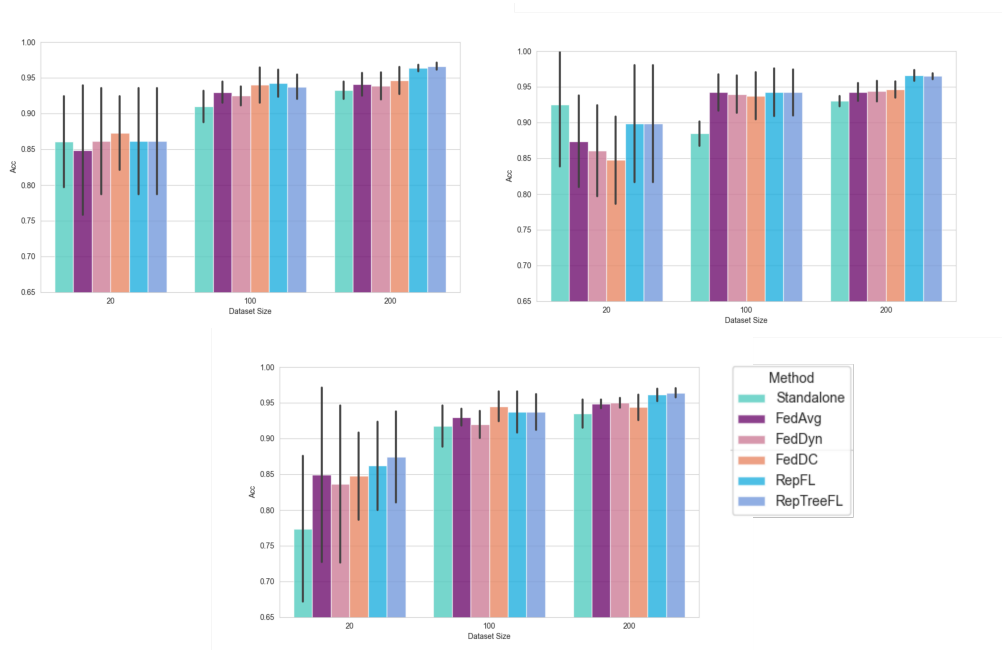


Figure 7: Accuracy analysis of different small dataset sizes on PneumoniaMNIST. Perturbation rate is $p = 10\%$, number of replicas is $r = 3$ and depth is $d = 1$.

fect of our proposed method, as the framework can be seen as related to ensemble methods.

When analysing the results on the graph generation task, there is a significant difference in MAE between our method and centralized training, as this task involves a higher level of complexity.

4.9. Computation and memory concerns

While replicas facilitate learning with limited data and a small amount of clients in federated learning, they are essentially duplicates of the original models and are stored at the anchor clients. This implies extra memory and computational resources, which needs to be considered in future work. One

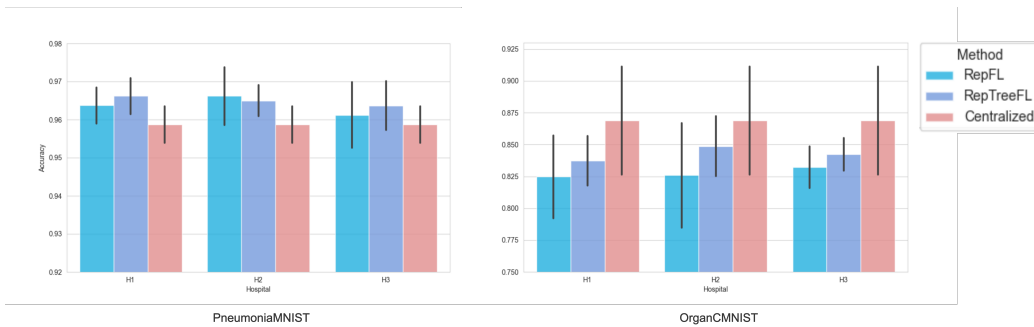


Figure 8: Accuracy comparison to centralized training on MedMNIST

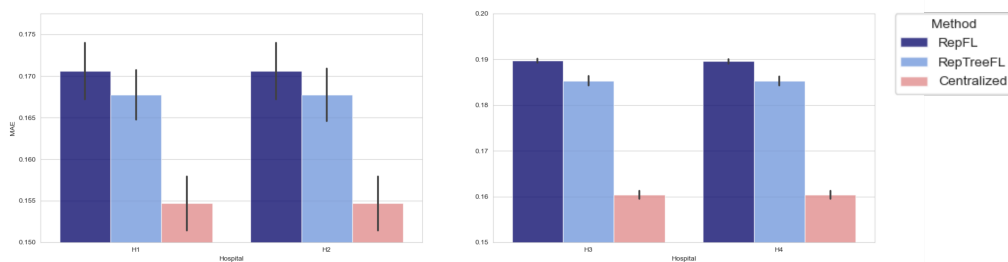


Figure 9: MAE comparison to centralized training. Clients H1 and H2 have as model G_1 , while H3 and H4 have architecture G_2 . The number of replicas is set to $r = 5$.

approach to minimise this concern is opting for a model architecture that is as simple as possible.

5. Conclusion

We proposed RepTreeFL, a novel framework for the limited data setting, where a small number of clients are participating in the federation process. The solution consists in replicating each original client and perturbing its local dataset, such that the model performance is enhanced by a larger amount of diverse clients. The method combines the tree structure of the client network, as well as the diversity across created replicas, and introduces a

diversity-based aggregation approach. Empirical evaluation shows the efficacy of the proposed method on two different settings: image classification with homogeneous models and graph generation with heterogeneous models. Additionally, we provide an analysis of the main hyperparameters, on the perturbation approach, as well as on datasets of variable sizes. Future work includes analysing more complex diversity metrics for aggregation, as well as evaluating the method on non-IID data and decreasing the compute and memory budgets.

Data Availability

The data used for the graph super-resolution task is confidential, while the data used for image classification is publicly available at <https://medmnist.com/>.

Code Availability

The implementation is available at <https://github.com/basiralab/RepTreeFL>.

Competing Interests

The authors declare no competing interests.

References

- Acar, D.A.E., Zhao, Y., Matas, R., Mattina, M., Whatmough, P., Saligrama, V., 2020. Federated learning based on dynamic regularization, in: International Conference on Learning Representations.
- Alam, S., Liu, L., Yan, M., Zhang, M., 2022. Fedrolex: Model-heterogeneous federated learning with rolling sub-model extraction. *Advances in Neural Information Processing Systems* 35, 29677–29690.
- Arivazhagan, M.G., Aggarwal, V., Singh, A.K., Choudhary, S., 2019. Federated learning with personalization layers. *arXiv preprint arXiv:1912.00818* .
- Bilic, P., Christ, P.F., et al., 2019. The liver tumor segmentation benchmark (lits). *CoRR* abs/1901.04056. [1901.04056](https://arxiv.org/abs/1901.04056).
- Caldas, S., Konečný, J., McMahan, H.B., Talwalkar, A., 2018. Expanding the reach of federated learning by reducing client resource requirements. *arXiv preprint arXiv:1812.07210* .
- Chlap, P., Min, H., Vandenberg, N., Dowling, J., Holloway, L., Haworth, A., 2021. A review of medical image data augmentation techniques for deep learning applications. *Journal of Medical Imaging and Radiation Oncology* 65, 545–563.
- Cinar, E., Haseki, S.E., Bessadok, A., Rekik, I., 2022. Deep cross-modality and resolution graph integration for universal brain connectivity mapping and augmentation, in: *MICCAI Workshop on Imaging Systems for GI Endoscopy*, Springer. pp. 89–98.

- Deng, Y., Kamani, M.M., Mahdavi, M., 2020. Adaptive personalized federated learning. arXiv preprint arXiv:2003.13461 .
- Diao, E., Ding, J., Tarokh, V., 2020. Heteroff: Computation and communication efficient federated learning for heterogeneous clients, in: International Conference on Learning Representations.
- Dosenbach, N.U., Nardos, B., Cohen, A.L., Fair, D.A., Power, J.D., Church, J.A., Nelson, S.M., Wig, G.S., Vogel, A.C., Lessov-Schlaggar, C.N., et al., 2010. Prediction of individual brain maturity using fmri. *Science* 329, 1358–1361.
- Ghilea, R., Rekik, I., 2023. Replica-based federated learning with heterogeneous architectures for graph super-resolution, in: International Workshop on Machine Learning in Medical Imaging, Springer. pp. 273–282.
- Ghosh, A., Chung, J., Yin, D., Ramchandran, K., 2020. An efficient framework for clustered federated learning. *Advances in Neural Information Processing Systems* 33, 19586–19597.
- Goodfellow, I., Pouget-Abadie, J., Mirza, M., Xu, B., Warde-Farley, D., Ozair, S., Courville, A., Bengio, Y., 2020. Generative adversarial networks. *Communications of the ACM* 63, 139–144.
- Gui, J., Sun, Z., Wen, Y., Tao, D., Ye, J., 2021. A review on generative adversarial networks: Algorithms, theory, and applications. *IEEE transactions on knowledge and data engineering* 35, 3313–3332.
- Hanzely, F., Richtárik, P., 2020. Federated learning of a mixture of global and local models. arXiv preprint arXiv:2002.05516 .

- He, C., Annavaram, M., Avestimehr, S., 2020. Group knowledge transfer: Federated learning of large cnns at the edge. *Advances in Neural Information Processing Systems* 33, 14068–14080.
- He, K., Zhang, X., Ren, S., Sun, J., 2016. Deep residual learning for image recognition, in: *Proceedings of the IEEE conference on computer vision and pattern recognition*, pp. 770–778.
- Hinton, G., Vinyals, O., Dean, J., 2015. Distilling the knowledge in a neural network. *arXiv preprint arXiv:1503.02531* .
- Horvath, S., Laskaridis, S., Almeida, M., Leontiadis, I., Venieris, S., Lane, N., 2021. Fjord: Fair and accurate federated learning under heterogeneous targets with ordered dropout. *Advances in Neural Information Processing Systems* 34, 12876–12889.
- Kairouz, P., McMahan, H.B., Avent, B., Bellet, A., Bennis, M., Bhagoji, A.N., Bonawitz, K., Charles, Z., Cormode, G., Cummings, R., et al., 2021. Advances and open problems in federated learning. *Foundations and Trends® in Machine Learning* 14, 1–210.
- Kamp, M., Fischer, J., Vreeken, J., 2022. Federated learning from small datasets, in: *The Eleventh International Conference on Learning Representations*.
- Kim, H.E., Cosa-Linan, A., Santhanam, N., Jannesari, M., Maros, M.E., Ganslandt, T., 2022. Transfer learning for medical image classification: a literature review. *BMC medical imaging* 22, 69.

- Kulkarni, V., Kulkarni, M., Pant, A., 2020. Survey of personalization techniques for federated learning, in: 2020 Fourth World Conference on Smart Trends in Systems, Security and Sustainability (WorldS4), IEEE. pp. 794–797.
- Li, D., Wang, J., 2019. Fedmd: Heterogenous federated learning via model distillation. arXiv preprint arXiv:1910.03581 .
- Li, T., Sahu, A.K., Zaheer, M., Sanjabi, M., Talwalkar, A., Smith, V., 2020. Federated optimization in heterogeneous networks. *Proceedings of Machine learning and systems* 2, 429–450.
- Litany, O., Maron, H., Acuna, D., Kautz, J., Chechik, G., Fidler, S., 2022. Federated learning with heterogeneous architectures using graph hypernetworks. arXiv preprint arXiv:2201.08459 .
- Liu, W., Wei, D., Chen, Q., Yang, W., Meng, J., Wu, G., Bi, T., Zhang, Q., Zuo, X.N., Qiu, J., 2017. Longitudinal test-retest neuroimaging data from healthy young adults in southwest china. *Scientific data* 4, 1–9.
- McMahan, B., Moore, E., Ramage, D., Hampson, S., y Arcas, B.A., 2017. Communication-efficient learning of deep networks from decentralized data, in: *Artificial intelligence and statistics*, PMLR. pp. 1273–1282.
- Mhiri, I., Mahjoub, M.A., Rekik, I., 2021. Stairwaygraphnet for inter- and intra-modality multi-resolution brain graph alignment and synthesis, in: *Machine Learning in Medical Imaging: 12th International Workshop, MLMI 2021, Held in Conjunction with MICCAI 2021, Strasbourg, France, September 27, 2021, Proceedings* 12, Springer. pp. 140–150.

- Sattler, F., Müller, K.R., Samek, W., 2020. Clustered federated learning: Model-agnostic distributed multitask optimization under privacy constraints. *IEEE transactions on neural networks and learning systems* 32, 3710–3722.
- Shamsian, A., Navon, A., Fetaya, E., Chechik, G., 2021. Personalized federated learning using hypernetworks, in: *International Conference on Machine Learning*, PMLR. pp. 9489–9502.
- Shen, X., Tokoglu, F., Papademetris, X., Constable, R., 2013. Groupwise whole-brain parcellation from resting-state fmri data for network node identification. *Neuroimage* 82, 403–415.
- Shorten, C., Khoshgoftaar, T.M., 2019. A survey on image data augmentation for deep learning. *Journal of big data* 6, 1–48.
- Simonovsky, M., Komodakis, N., 2017. Dynamic edge-conditioned filters in convolutional neural networks on graphs, in: *Proceedings of the IEEE conference on computer vision and pattern recognition*, pp. 3693–3702.
- Tan, A.Z., Yu, H., Cui, L., Yang, Q., 2022. Towards personalized federated learning. *IEEE Transactions on Neural Networks and Learning Systems* .
- Torrey, L., Shavlik, J., 2010. Transfer learning, in: *Handbook of research on machine learning applications and trends: algorithms, methods, and techniques*. IGI global, pp. 242–264.
- Xu, X., Zhou, F., et al., 2019. Efficient multiple organ localization in ct image using 3d region proposal network. *IEEE Transactions on Medical Imaging* 38, 1885–1898.

- Yang, J., Shi, R., Ni, B., 2021. Medmnist classification decathlon: A lightweight automl benchmark for medical image analysis, in: IEEE 18th International Symposium on Biomedical Imaging (ISBI), pp. 191–195.
- Yang, J., Shi, R., Wei, D., Liu, Z., Zhao, L., Ke, B., Pfister, H., Ni, B., 2023. Medmnist v2-a large-scale lightweight benchmark for 2d and 3d biomedical image classification. *Scientific Data* 10, 41.
- Zhang, M., Sapra, K., Fidler, S., Yeung, S., Alvarez, J.M., 2021. Personalized federated learning with first order model optimization. [2012.08565](#).
- Zhuang, F., Qi, Z., Duan, K., Xi, D., Zhu, Y., Zhu, H., Xiong, H., He, Q., 2020. A comprehensive survey on transfer learning. *Proceedings of the IEEE* 109, 43–76.

Appendix A. Mathematical Notations

Table A.5: Table of mathematical notations

Notation	Dimension	Description
m	1	Number of original clients
i	1	Indicator for client
D_i	1	Local dataset of client i
n_i	1	Length of the dataset of client i
r_i	1	Number of replicas of client i
p_i	1	Perturbation rate (percentage) of client i
d_i	1	Maximum replica depth of client i
j	1	Indicator for sample
$X_{i,j}$	\mathbb{R}^2	Image j of client i
$y_{i,j}$	1	Label of sample j of client i
$X_{i,j}^s$	\mathbb{R}^2	Source brain graph from sample j of client i
$X_{i,j}^t$	\mathbb{R}^2	Target brain graph from sample j of client i
X^s	\mathbb{R}^2	Set of source brain graphs on anchor
X^t	\mathbb{R}^2	Set of target brain graphs on anchor
$X^{s'}$	\mathbb{R}^2	Set of source brain graphs on replica at $d = 1$
$X^{t'}$	\mathbb{R}^2	Set of target brain graphs on replica at $d = 1$
$X^{s''}$	\mathbb{R}^2	Set of source brain graphs on replica at $d = 2$
$X^{t''}$	\mathbb{R}^2	Set of target brain graphs on replica at $d = 2$
a	1	Anchor index
r	1	Replica index
α	\mathbb{R}	Aggregation weights
G_1	-	Generator 1
G_2	-	Generator 2
n_c	1	Number of common layers between two heterogeneous models
W^C	$n_c \times \mathbb{R}^2$	Weight matrices of common layers between two heterogeneous models